Doping dependence of the optical properties of low-dimensional perovskite-related La1−yCayTiO3.4±δ

Komalavalli Thirunavukkuarasu, Frank Lichtenberg, Christine A. Kuntscher

Angaben zur Veröffentlichung / Publication details:

Thirunavukkuarasu, Komalavalli, Frank Lichtenberg, and Christine A. Kuntscher. 2006. "Doping dependence of the optical properties of low-dimensional perovskite-related La1−yCayTiO3.4±δ." *Journal of Physics: Condensed Matter* 18 (40): 9173–87. https://doi.org/10.1088/0953-8984/18/40/004.

Doping dependence of the optical properties of low-dimensional perovskite-related $La_{1-y}Ca_yTiO_{3.4\pm\delta}$

K Thirunavukkuarasu[1], **F Lichtenberg**[2] **and C A Kuntscher**[1,3]

[1] 1.Physikalisches Institut, Universität Stuttgart, Pfaffenwaldring 57, D-70550 Stuttgart, Germany
[2] Experimentalphysik VI, Institut für Physik, EKM, Universität Augsburg, Universitätsstrasse 1, D-86135 Augsburg, Germany

E-mail: christine.kuntscher@physik.uni-augsburg.de

Abstract

The doping dependence of the optical properties of $La_{1-y}Ca_yTiO_{3.4\pm\delta}$ crystals was studied by polarization-dependent infrared reflectivity measurements at room temperature. For $y < 0.2$ the optical conductivity spectra reveal a quasi-one-dimensional conducting character, and the phonon spectra suggest small changes in the crystal structure and effective charge induced by the substitution of trivalent lanthanum with divalent calcium. The pronounced mid-infrared absorption band observed along the conducting direction shifts to lower frequencies with increasing electron concentration. The possible origin of the band is discussed in terms of polaronic excitations, Mott–Hubbard excitations, phonon-assisted Ti t_{2g} d–d transitions, and charge-transfer (2p–3d) transitions. Among these interpretations the polaron model is most likely. $La_{1-y}Ca_yTiO_{3.4\pm\delta}$ with $y = 0.2$ and $\delta = 0$ exhibits an insulating character and a less anisotropic optical response. The observed differences in the electronic and vibrational excitations in $La_{0.8}Ca_{0.2}TiO_{3.40}$ compared to the other studied titanates could be due to local changes of the crystal structure.

1. Introduction

The interplay of the various degrees of freedom in perovskite titanates leads to interesting ground states [1–6]. As an example, the compound $LaTiO_{3.0}$ is intensively studied and the possibility of an orbitally ordered versus an orbital liquid state is under debate. $LaTiO_{3.0}$ belongs to the titanate series (La, Ca)$TiO_{3.5-x}$ with $0 \leqslant x \leqslant 0.5$, which comprises compounds with a wide range of properties, including the antiferromagnetic Mott–Hubbard insulator

[3] Present address: Lehrstuhl für Experimentalphysik II, Universität Augsburg, Universitätsstr. 1, 86159 Augsburg, Germany.

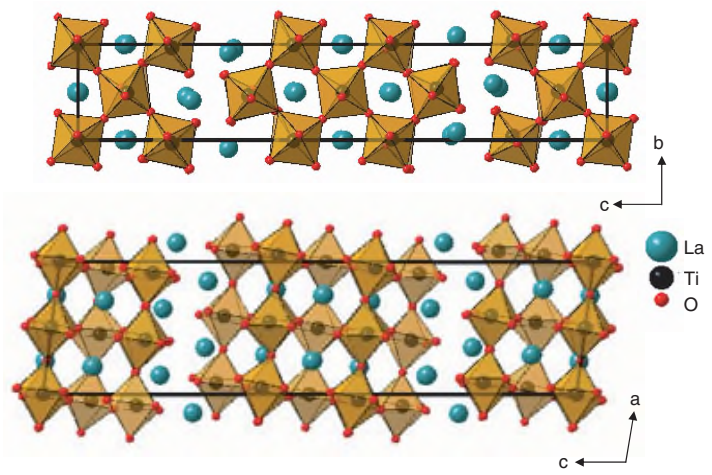

Figure 1. Crystal structure of $LaTiO_{3.41}$ viewed along the a axis (top) and along the b axis (bottom), illustrating the anisotropic character with chains of TiO_6 octahedra along the a axis [17].

$LaTiO_{3.0}$, the ferroelectric band insulator $LaTiO_{3.5}$, and (semi)conducting compounds for intermediate oxygen contents, $0 < x < 0.5$ [7]. In particular, $LaTiO_{3.41}$ is a quasi-one-dimensional (quasi-1D) conductor according to dc resistivity [7] and infrared reflectivity measurements [8]. The optical conductivity spectrum of $LaTiO_{3.41}$ for the polarization along the conducting a axis contains a pronounced absorption band in the mid-infrared (MIR) frequency range with a strong temperature dependence. It was proposed that this MIR band is due to the excitation of vibrational polarons [8], and thus suggests the importance of electron–phonon coupling in this series of compounds. On the other hand, electronic correlations in general play an important role in the conduction mechanism of 3d transition metal oxides, and also need to be considered. The dominant mechanism determining the electronic properties of $LaTiO_{3.41}$ is still an open issue [9, 10].

As demonstrated in other low-dimensional systems, like the 1D metal β-$Na_{0.33}V_2O_5$ [11, 12], the 2D organic conductor κ-$(BEDT\text{-}TTF)_2Cu(NCS)_2$ [13], and the 2D cuprates [14–16], the MIR absorption band contains significant information about the conduction mechanism. Besides the temperature dependence, the doping dependence of the MIR band was shown to be an important criterion to unravel its character. Hence, also in the case of the titanate series (La, Ca) $TiO_{3.5-x}$ the effect of electron doping on the MIR band is expected to give further indications for the possible existence of polaronic carriers. Therefore, we studied the optical properties of various crystals $La_{1-y}Ca_yTiO_{3.4\pm\delta}$ with $0 \leqslant y \leqslant 0.2$ and $0 \leqslant \delta \leqslant 0.05$, i.e., with different electron densities, in the infrared frequency range.

The investigated systems are $A_nB_nO_{3n+2}$ perovskite-related compounds of the type $n = 5$ [7]. As an example, we show in figure 1 the monoclinic crystal structure (belonging to space group $P2_1/c$) of $LaTiO_{3.41}$, which consists of slabs of vertex-sharing TiO_6 octahedra [17]. The slabs are five octahedra wide along the c direction, and neighbouring slabs are offset by half an octahedron along the a axis. Furthermore, the octahedra are rotated around the a axis and tilted. Due to the complex crystal structure, the number of formula units in the monoclinic unit cell is large (20); therefore, the unit cell comprises altogether 108 atoms.

In this manuscript we present the polarization-dependent optical response of $La_{1-y}Ca_yTiO_{3.4\pm\delta}$ compounds with different electron doping levels. Of particular interest is

Table 1. Lattice parameters of the studied $La_{1-y}Ca_yTiO_{3.4\pm\delta}$ crystals [7, 17, 18]. Also listed is the nominal number $N_{nominal}$ of Ti 3d electrons for each compound together with the effective number N_{eff} of free electrons per formula unit for each compound, calculated according to the sum rule given by equation (1), and the ratio of the effective number of electrons N_{eff} to the nominal number of electrons $N_{nominal}$.

Single crystal	a (Å)	b (Å)	c (Å)	β	$N_{nominal}$	N_{eff}	$N_{eff}/N_{nominal}$
$La_{0.965}TiO_{3.35}$	7.86	5.53	31.47	97.1	0.195	0.110 16	0.565
$LaTiO_{3.41}$	7.86	5.53	31.45	97.2	0.18	0.102 32	0.568
$La_{0.89}Ca_{0.11}TiO_{3.36}$	7.84	5.52	31.09	96.1	0.17	0.093 54	0.550
$La_{0.9}Ca_{0.1}TiO_{3.38}$	7.83	5.52	31.1	96.2	0.14	0.080 52	0.575
$La_{0.87}Ca_{0.13}TiO_{3.39}$	7.83	5.52	31.05	96.2	0.09	0.058 6	0.651
$La_{0.8}Ca_{0.2}TiO_{3.40}$	7.79	5.52	31.5	97.0	0	—	—

the doping dependence of the MIR absorption band, which gives insight into its character. Besides excitations of polaronic character, purely electronic excitations—like Mott–Hubbard inner-gap states, local crystal field excitations, and charge-transfer excitations—are considered as an explanation for the MIR band. Furthermore, differences in phonon spectra are briefly discussed.

2. Experiment

$La_{1-y}Ca_yTiO_{3.4\pm\delta}$ crystals were synthesized by a floating zone melting process and their compositions were determined by thermogravimetric oxidation [7]. In table 1 the investigated $La_{1-y}Ca_yTiO_{3.4\pm\delta}$ crystals are listed with their lattice parameters [7, 17, 18]. They all have comparable lattice parameters, with the most significant differences in the c axis parameter and monoclinic angle β. The nominal number $N_{nominal}$ of Ti 3d valence electrons is calculated assuming an ionic picture and valences -2 and $+3$ of the oxygen and lanthanum ions, respectively.

The investigated titanate samples were polished on a polishing disc using diamond paste with a grain size of 1 μm to obtain flat and shiny surfaces. The polarization-dependent reflectivity spectra of $La_{1-y}Ca_yTiO_{3.4\pm\delta}$ for the electric field $\mathbf{E}$ of the incident radiation along the a and b axes were measured at room temperature in the frequency range 50–12 000 cm^{-1} using a Fourier-transform spectrometer (Bruker IFS 66v/S) in combination with an infrared microscope. The infrared microscope enables the study of spots on the sample with a diameter of only a few tens of micrometres. Thus, we could probe several positions on the sample and verify its homogeneity. In order to obtain the absolute reflectivity, the intensity spectrum reflected from an aluminium mirror was used as reference. All reflectivity spectra were fitted with the Drude–Lorentz model. Based on these fits, the spectra were extrapolated to low ($\omega = 0$) and high frequencies ($\omega = 100\,000$ cm^{-1}), thereby also taking into account the high-frequency data (up to 36 000 cm^{-1}) of $LaTiO_{3.41}$ recorded with a variable angle spectroscopic ellipsometer [19]. By the subsequent Kramers–Kronig transformation the frequency-dependent optical conductivity σ_1 was calculated.

3. Results

The polarization-dependent reflectivity and optical conductivity spectra of the studied titanates are shown in figures 2 and 3, respectively. For $\mathbf{E} \parallel a$ the $La_{1-y}Ca_yTiO_{3.4\pm\delta}$ compounds with $y < 0.2$ show a metallic-like increase of the reflectivity with decreasing frequency in the low-frequency range ($\leqslant$110 cm^{-1}) and a Drude-like contribution, superimposed by phonon

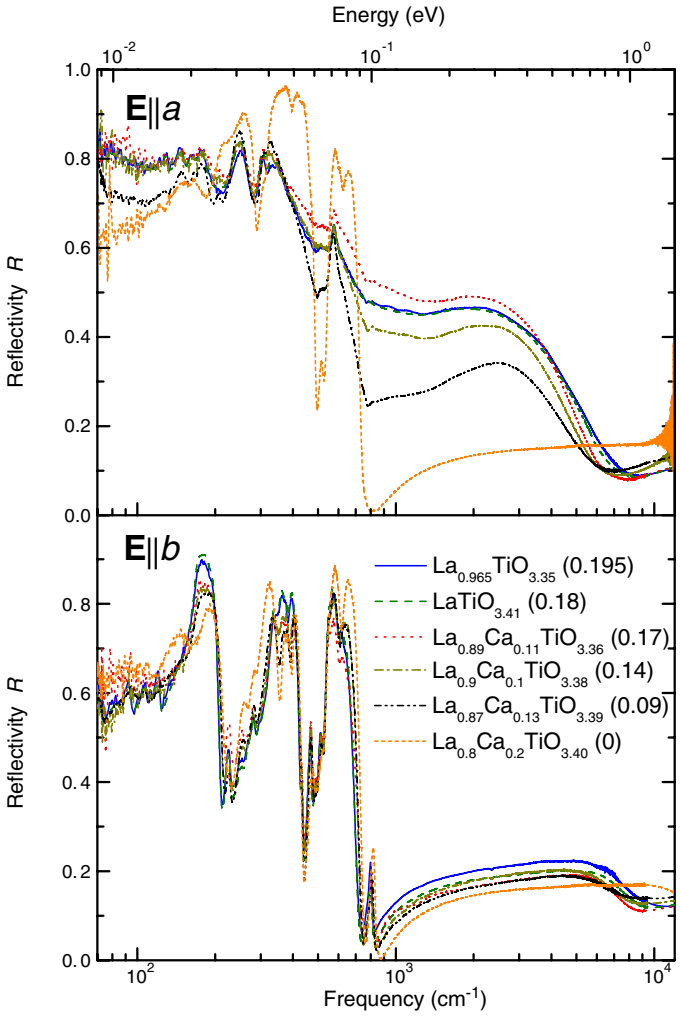

Figure 2. Reflectivity R of $La_{1-y}Ca_yTiO_{3.4\pm\delta}$ crystals for the polarizations $\mathbf{E} \parallel a$ and $\mathbf{E} \parallel b$ at room temperature. The nominal number N_{nominal} of Ti 3d electrons is given in parenthesis for each compound.

lines, in the corresponding optical conductivity spectra. A characteristic feature of the $\mathbf{E} \parallel a$ optical conductivity is a pronounced absorption band centred at around 2500 cm^{-1}. For $\mathbf{E} \parallel b$ the overall reflectivity is lower, and in the optical conductivity spectra only strong phonon excitations are found in the far-infrared range, indicating an insulating character; at higher frequencies ($\approx$6000 cm^{-1}) an absorption band is observed, which we assign to charge-transfer excitations.

The most pronounced changes with electron doping are seen in the $\mathbf{E} \parallel a$ spectra: for low doping levels ($N_{\mathrm{nominal}} = 0.09, 0$) the low-frequency ($\leqslant$200 cm^{-1}) reflectivity is significantly reduced, and for $La_{0.8}Ca_{0.2}TiO_{3.40}$ it even decreases with decreasing frequency, indicating an insulating character. Correspondingly, in the optical conductivity spectra the Drude term is gradually suppressed with decreasing electron doping and has disappeared for $La_{0.8}Ca_{0.2}TiO_{3.40}$. Pronounced changes are also found in the MIR range, where the broad

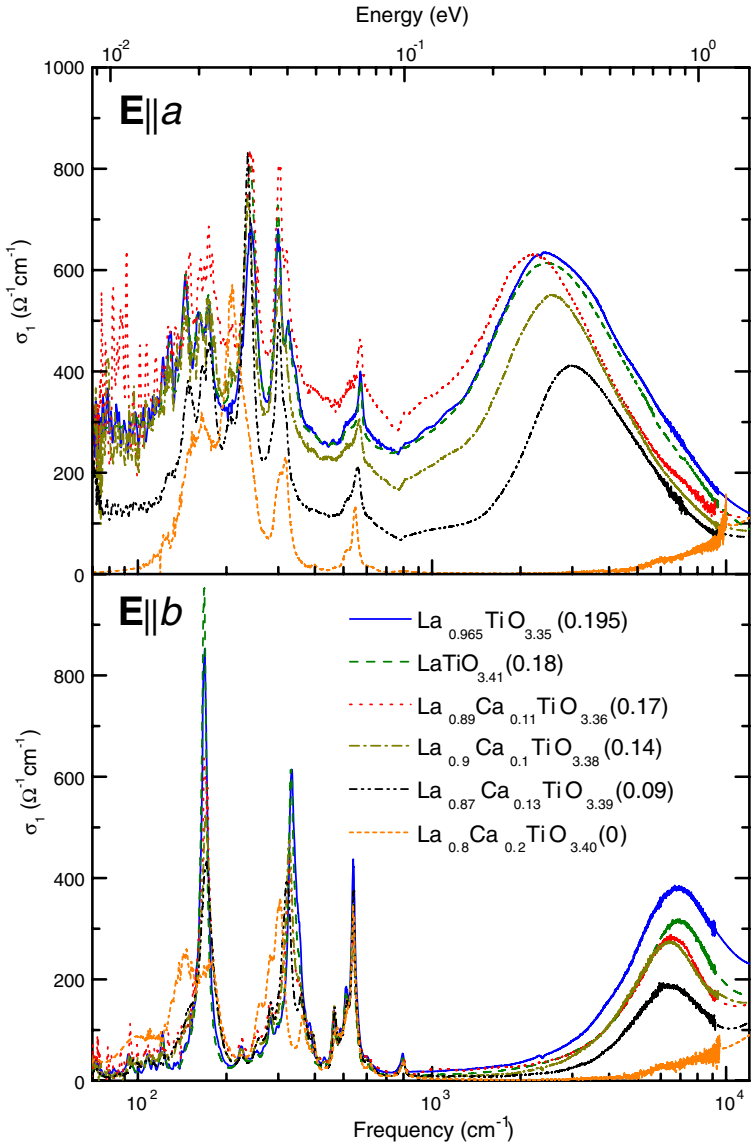

Figure 3. Optical conductivity σ_1 of $La_{1-y}Ca_yTiO_{3.4\pm\delta}$ crystals for $\mathbf{E} \parallel a$ and $\mathbf{E} \parallel b$ at room temperature, obtained from Kramers–Kronig transformation. The nominal number N_{nominal} of Ti 3d electrons is given in parenthesis for each compound.

absorption band is located (see figure 3). The position and intensity of the band depends on the electron doping level. The MIR band shifts to lower frequencies and its intensity increases with increasing electron density. For $La_{0.8}Ca_{0.2}TiO_{3.40}$ ($N_{\text{nominal}} = 0$), the absorption bands in the optical conductivity for both $\mathbf{E} \parallel a$ and $\mathbf{E} \parallel b$ are absent.

The optical conductivity spectra along both a and b axes contain several phonon modes below 1000 cm^{-1}. The phonon spectra are shown in figure 4. For $\mathbf{E} \parallel a$ they were obtained by subtracting the MIR absorption band and the Drude contribution, obtained from the Drude–Lorentz fits, from the total optical conductivity. The phonon modes belong to three groups

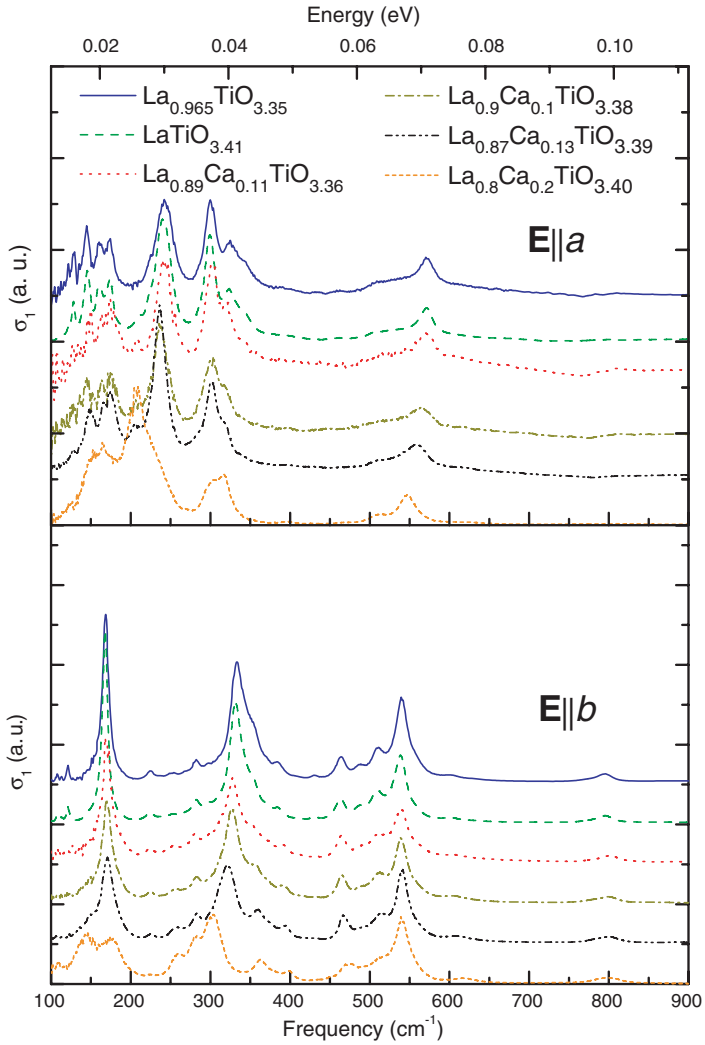

Figure 4. Phonon spectra of $La_{1-y}Ca_yTiO_{3.4\pm\delta}$ crystals for $\mathbf{E} \parallel a$ and $\mathbf{E} \parallel b$. The spectra are shifted for clarity.

located in the following ranges: 100–200 cm^{-1}, 200–400 cm^{-1}, and 400–850 cm^{-1}. Based on a comparison with typical perovskite materials like $LaTiO_3$ [20] and $BaTiO_3$ [21], they can be assigned to external vibrational modes of the TiO_6 octahedra against the cations (La^{3+}/Ca^{2+} ions) and the TiO_6 octahedral bending and stretching modes, respectively. The resonance frequencies of the phonon modes were extracted from the optical conductivity spectra by fitting with the Drude–Lorentz model and are listed in table 2.

The phonon spectra for the titanates $La_{0.965}TiO_{3.35}$ ($N_{\mathrm{nominal}} = 0.195$) and $LaTiO_{3.41}$ ($N_{\mathrm{nominal}} = 0.18$) are very similar, with small differences in the oscillator strengths. However, doping causes changes which are illustrated in figure 5: here we compare the phonon modes with those of $La_{0.965}TiO_{3.35}$, i.e., the studied titanate with the highest electron doping level. The relative shifts $\Delta\omega_j/\omega_{j,\mathrm{La_{0.965}TiO_{3.35}}}$, with $\Delta\omega_j = \omega_j - \omega_{j,\mathrm{La_{0.965}TiO_{3.35}}}$, of the phonon modes with respect to $La_{0.965}TiO_{3.35}$ are presented as a function of calcium content y. For the polarization

Table 2. Frequencies of the main phonon modes in cm^{-1} of the $La_{1-y}Ca_yTiO_{3.4\pm\delta}$ crystals for $\mathbf{E} \parallel a$ and $\mathbf{E} \parallel b$, obtained from the Drude–Lorentz fits of the spectra shown in figure 4. The strongest modes are indicated by (s).

$La_{0.965}TiO_{3.35}$	$LaTiO_{3.41}$	$La_{0.89}Ca_{0.11}TiO_{3.36}$	$La_{0.9}Ca_{0.1}TiO_{3.38}$	$La_{0.87}Ca_{0.13}TiO_{3.39}$	$La_{0.8}Ca_{0.2}TiO_{3.40}$
			$\mathbf{E} \parallel a$		
162	161	163	164	165	165
174	173	176	176	175	182
—	209	208	205	206	208 (s)
239 (s)	237 (s)	237 (s)	237 (s)	238 (s)	237
300 (s)	299 (s)	302 (s)	301 (s)	301	303
325	324	321	320	318	318
571	570	569	566	558	547
			$\mathbf{E} \parallel b$		
—	—	143	145	147	145
167 (s)	167 (s)	170 (s)	171 (s)	172 (s)	177
282	282	281	283	283	282
333 (s)	330 (s)	328 (s)	327 (s)	321 (s)	304 (s)
353	355	357	358	361	364
385	386	391	392	394	397
463	464	465	466	467	468
509	509	510	513	513	512
540 (s)	540 (s)	539 (s)	539 (s)	541 (s)	541 (s)
795	795	796	800	801	800

$\mathbf{E} \parallel a$ some changes with increasing calcium content are observed for the modes at 174 and 571 cm^{-1}, which shift to higher and lower frequencies, respectively. The strong phonon mode around 300 cm^{-1} is gradually damped (see figure 4). Moreover, there seems to be a redistribution of oscillator strength between the phonon modes located at 237 and 208 cm^{-1} for the compound $La_{0.8}Ca_{0.2}TiO_{3.40}$.

Changes in the phonon spectra due to calcium doping are most pronounced along the b axis: regarding the external vibrational modes, the strongest line at 167 cm^{-1} shifts to higher frequencies and its intensity decreases with increasing calcium doping y. Furthermore, an additional phonon mode gradually develops at around 145 cm^{-1}. The TiO_6 bending modes (200–400 cm^{-1}) also show considerable changes: the main phonon mode at 333 cm^{-1}, which is almost constant for the titanates $La_{0.965}TiO_{3.35}$ and $LaTiO_{3.41}$, shifts to lower frequencies, while the phonons at 353 and 385 cm^{-1} harden with increasing calcium content. The octahedral stretching modes are almost unaffected by the doping; only the relatively weak mode at 509 cm^{-1} is gradually damped.

4. Discussion

Information about subtle differences in the crystal structure of the different $La_{1-y}Ca_yTiO_{3.4\pm\delta}$ compounds can be inferred from a comparison of the phonon spectra. Calcium doping causes changes in the phonon spectra, in particular for $\mathbf{E} \parallel b$, as illustrated in figure 5. With increasing calcium doping the strong phonon line centred at 167 cm^{-1}, which is related to the external vibrational modes, shifts to higher frequencies by nearly 6% and its intensity decreases. Also the external vibrational modes for $\mathbf{E} \parallel a$, located at 162 and 174 cm^{-1}, exhibit shifts to higher frequencies. The shifts of the phonon modes for the polarization $\mathbf{E} \parallel a$ are smaller

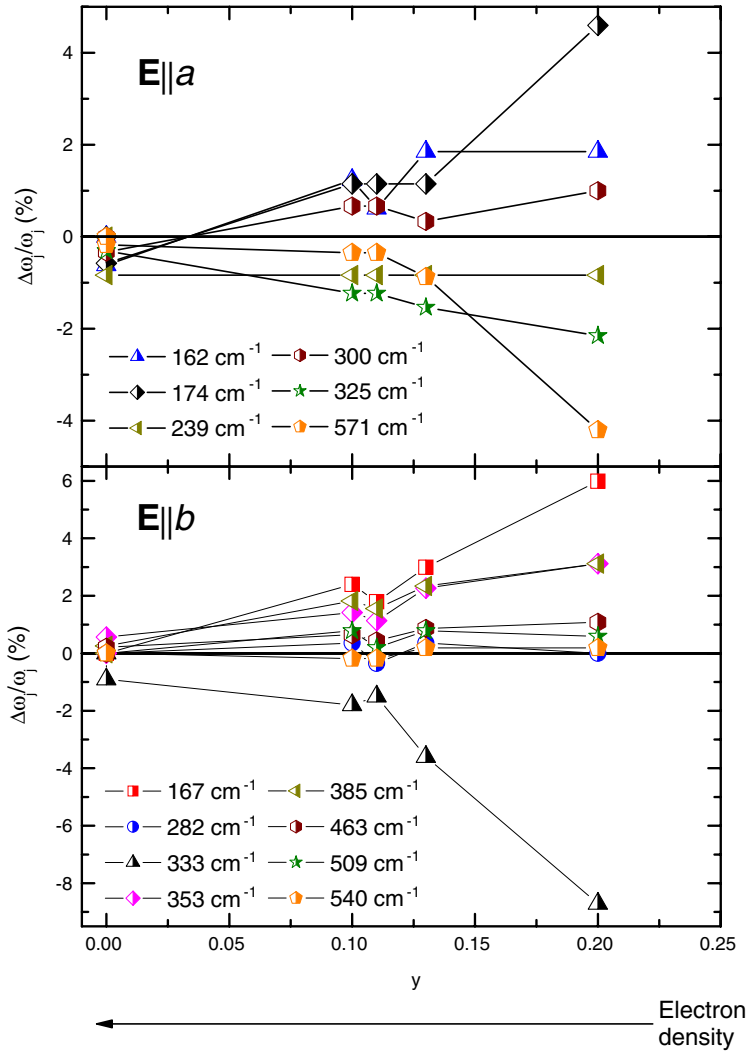

Figure 5. Relative shifts $\Delta\omega_j/\omega_j$ of the $\mathbf{E} \parallel a$ and $\mathbf{E} \parallel b$ phonon modes for $La_{1-y}Ca_yTiO_{3.4\pm\delta}$ crystals with respect to $La_{0.965}TiO_{3.35}$ (see text) as a function of calcium content y and electron density. The frequencies in the legend correspond to the phonon modes in $La_{0.965}TiO_{3.35}$.

compared to those for $\mathbf{E} \parallel b$. The largest changes (>4%) are found for the insulating material $La_{0.8}Ca_{0.2}TiO_{3.4}$ with the highest calcium content. In general, the frequency ω_j of a vibrational mode is related to the reduced mass m of the ions involved in the vibration according to $\omega_j = \sqrt{k_j/m_j}$, where k_j is the force constant of the mode [22]. Accordingly, the external vibrational modes, where the TiO_6 octahedra oscillate against the anion, are expected to shift to higher frequencies when heavier La^{3+} ions are substituted by lighter Ca^{2+} ions, in agreement with our findings.

Although the simple mass consideration qualitatively explains the shift in frequency of the vibrational mode, it cannot explain the damping of the strongest phonon as well as the appearance of a new phonon in the lower frequency range around 145 cm^{-1} for $\mathbf{E} \parallel b$. The calcium doping furthermore causes frequency shifts and changes in oscillator strengths for

several other modes, and the appearance of new lines in the bending and the stretching modes of the TiO_6 octahedra. In particular, the central group of phonons which corresponds to the bending mode of the TiO_6 octahedra splits into several lines along both studied directions. Since the crystal structure parameters are only slightly altered by calcium doping (see table 1), these changes in the phonon modes could be attributed to small distortions of the TiO_6 octahedra and changes in the bond lengths, which were found to greatly influence the vibrational modes in several rare-earth and alkali-metal titanates [21, 23–25]. Furthermore, the role of effective charge cannot be neglected as we substitute La^{3+} by Ca^{2+}, since it generally influences the force constant of the vibrational modes [21]. The study on titanate perovskites (especially ferroelectric titanates) has also shown that the amplitude of effective charge is dependent on the particular interatomic distance and crucially affected by the anisotropy of Ti environment along the Ti–O chains [26].

An interesting feature in the optical conductivity spectra of $La_{1-y}Ca_yTiO_{3.4\pm\delta}$ with $y < 0.2$ for the polarization along the conducting a axis is a pronounced MIR band. In the case of $LaTiO_{3.41}$ it was proposed that this band is due to the photoionization of polaronic charge carriers [8–10]. From the temperature dependence of the MIR band position in $LaTiO_{3.41}$, which is—within a polaronic scenario—directly linked to the polaron binding energy [27], a picture of independent small polarons appeared less probable; rather, a model of interacting polaronic quasiparticles seemed to apply [8]. In this case, the position of the MIR band should depend on the density of the charge carriers, i.e. the doping level: with increasing electron doping the effective electron–phonon coupling is decreased due to increasing electron–electron interactions, thus decreasing the polaron binding energy [28, 29]. This fact was for example used to identify the nature of the polaronic band in the cuprate superconductors $Nd_{2-x}Ce_xCuO_{4-y}$ [16]. Therefore, the study of the doping dependence of the MIR band could provide an insight into the conduction mechanism in the $La_{1-y}Ca_yTiO_{3.4\pm\delta}$ compounds as well. From the optical properties of $La_{1-y}Ca_yTiO_{3.4\pm\delta}$ with $y < 0.2$, a dependence of the position of the MIR band on the carrier doping level is obvious: with increasing 3d electron number the MIR band shifts to lower frequencies. The MIR band of the studied $La_{1-y}Ca_yTiO_{3.4\pm\delta}$ compounds, extracted from the Drude–Lorentz fit of the optical conductivity, is shown in figure 6. Such a redshift of the MIR band is indeed compatible with an interacting polaron model [28–31].

Assuming that in the titanates $La_{1-y}Ca_yTiO_{3.4\pm\delta}$ polarons exist, a further open issue is their nature, i.e., whether they are small or large. A first hint can be inferred from the mobilities of the charge carriers, which are expected to be quite different for small and large polaronic quasiparticles. Large polarons move with large mobilities, $\mu > 1\ \mathrm{cm^2\ V^{-1}\ s^{-1}}$, in contrast to small polarons with $\mu < 1\ \mathrm{cm^2\ V^{-1}\ s^{-1}}$ [27]. The mobility μ of charge carriers can be roughly estimated from the dc conductivity σ_{dc} and the number n of electrons per unit volume according to $\mu = \sigma_{dc}/(n \cdot e)$, with e being the electron charge. From the dc conductivity σ_{dc} at 300 K ($1149\ \Omega^{-1}\ \mathrm{cm^{-1}}$) [8], the nominal number of electrons per unit cell (3.6 electrons/unit cell), and the volume of the unit cell ($1357\ \mathrm{\AA^3}$), the mobility μ of the compound $LaTiO_{3.41}$ was estimated to be $2.7\ \mathrm{cm^2\ V^{-1}\ s^{-1}}$. This value lies close to the limit between the large and small polaron regimes.

In order to check the reliability of this estimation based on the nominal number of electrons, the effective number of carriers obtained from the optical conductivity data was used in the calculation of the mobility. According to the sum rule, the effective number of valence electrons per formula unit, N_{eff}, is obtained by integrating the optical conductivity:

$$N_{eff} = \frac{2m_e V}{\pi e^2 Z} \int_0^{\omega_m} \sigma_1(\omega)\, \mathrm{d}\omega, \tag{1}$$

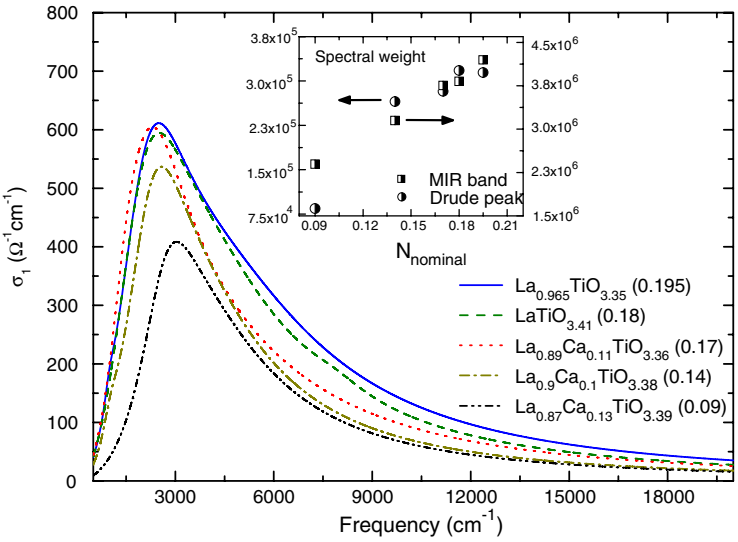

Figure 6. MIR absorption band of $La_{1-y}Ca_yTiO_{3.4\pm\delta}$ for $\mathbf{E} \parallel a$ extracted by Drude–Lorentz fits of the optical conductivity spectra. Inset: spectral weights of the Drude term and MIR band as a function of the nominal number of electrons N_{nominal}.

where m_e is the free electron mass, V is the volume of the unit cell, and Z is the number of formula units per unit cell. The upper integration limit ω_m was set to be 15 000 cm^{-1}, which is the approximate onset frequency of the interband transition. The phonon contribution was subtracted from the integrated total conductivity. N_{eff} calculated according to equation (1) qualitatively agrees with N_{nominal}: it follows the same tendency with calcium doping and is of the same order of magnitude as N_{nominal}, differing by a factor of about 0.6 for all studied compounds (see table 1). Using the so-obtained N_{eff} we estimate a mobility of 4.8 $\text{cm}^2\ \text{V}^{-1}\ \text{s}^{-1}$ for $LaTiO_{3.41}$. Furthermore, taking into account the low-frequency limit ($\omega \to 0$) of the optical conductivity in the calculation of mobility gives a value of 1.0 $\text{cm}^2\ \text{V}^{-1}\ \text{s}^{-1}$, which still lies in the limit between the large and small polaron regimes. Thus, based on estimation of the mobility of the titanate compounds, a distinction between the small and large polaron regimes is not possible.

Further insight into the nature of the polarons is given by the shape of the MIR absorption band [32, 33]. For large polarons the optical conductivity due to the photo-ionization of the charge carriers from self-trapped into free-carrier states is described by [27, 32]

$$\sigma_1(\omega) = n_p \frac{64}{3} \frac{e^2}{m} \frac{1}{\omega} \frac{(k(\omega)R)^3}{[1 + (k(\omega)R)^2]^4}, \tag{2}$$

where n_p is the polaron density, R is the polaron radius, and m and k are the mass and wavevector of the photoionized carrier, respectively. The wavevector is defined as $k = \sqrt{2m(\hbar\omega - 3E_p)}/\hbar$, where E_p is the ground state energy of a large polaron. The threshold energy for the photoionization amounts to $3E_p$.

Explicit analytical expressions for the frequency dependence of the optical conductivity due to photo-assisted hopping of small polarons were obtained in [34]. At temperatures $T \geqslant \omega_0/2k_B$, where ω_0 is the average frequency of the phonons to which the electrons couple,

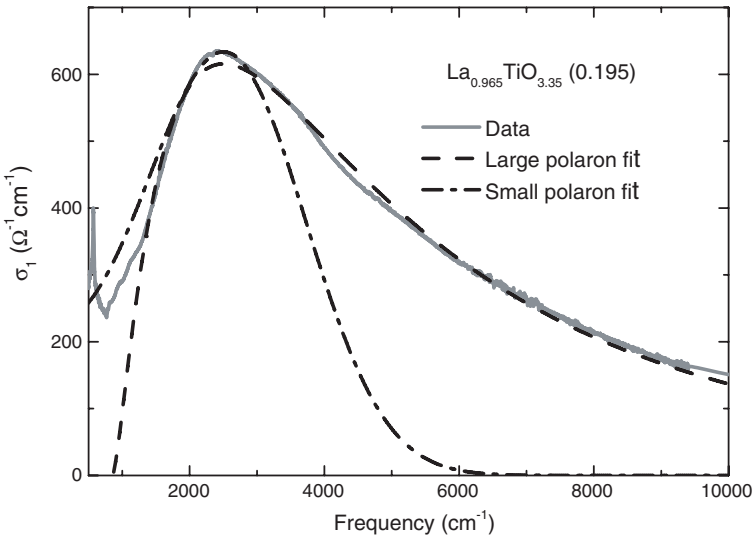

Figure 7. MIR absorption band of $La_{0.965}TiO_{3.35}$ for $\mathbf{E} \parallel a$ together with the results from the fitting with large and small polaron models according to equations (2) and (3), respectively.

the optical conductivity σ_1 is described by [34, 35]

$$\sigma_1(\omega, \beta) = \sigma(0, \beta)\frac{\sinh(\frac{1}{2}\omega\beta)}{\frac{1}{2}\omega\beta}\exp\left[-\frac{\beta\omega^2}{16E_a}\right], \tag{3}$$

where $\beta = 1/(k_B T)$, and E_a is the activation energy for hopping conduction of the carrier across the potential barrier and equals $E_b/2$, with E_b being the polaron binding energy.

The MIR bands in the optical conductivity spectra of the studied titanates were fitted with equations (2) and (3) for large and small polarons, respectively. The fitting parameters are the polaron density n_P, the polaron radius R, and the polaron energies E_p and E_a. The effective large polaron mass m was assumed to be equal to the free electron mass. As an example, the fits of the optical conductivity of $La_{0.965}TiO_{3.35}$ with the large and small polaron models together with the measured spectrum are shown in figure 7. For the large polaron model the parameters $n_P = 9.18 \times 10^{20}$ cm^{-3}, $E_p = 284.5$ cm^{-1}, and $R = 2.23$ Å, give the best fit. The so-obtained value of the polaron density n_P is in good agreement with the effective number N_{eff} of carriers given by the sum rule[3], indicating that our assumption of the effective large polaron mass being approximately equal to the free electron mass is reasonable. The polaron binding energy E_b and the dc conductivity $\sigma(0, \beta)$ from the small polaron fit amounts to 1499 and 226.5 Ω^{-1} cm^{-1}, respectively. Obviously, the large polaron model describes the asymmetric line-shape of the MIR band reasonably well, while for the small polaron model large discrepancies exist in the high-frequency part of the band. The radius, density, and ground state energy of the large polarons extracted from the large polaron fit are shown in figure 8 as a function of the nominal number of carriers $N_{nominal}$. The polaron density increases with increasing carrier doping as one would expect; the values obtained from the fits have the same order of magnitude as the nominal carrier density. The ground state polaron energy E_p, which indicates the threshold energy for the photoionization of the large polarons, decreases with increasing electron doping.

[3] For $La_{0.965}TiO_{3.35}$ the number of carriers per formula unit amounts to 0.11 (see table 1), which corresponds to a carrier density of 1.6×10^{21} cm^{-3}.

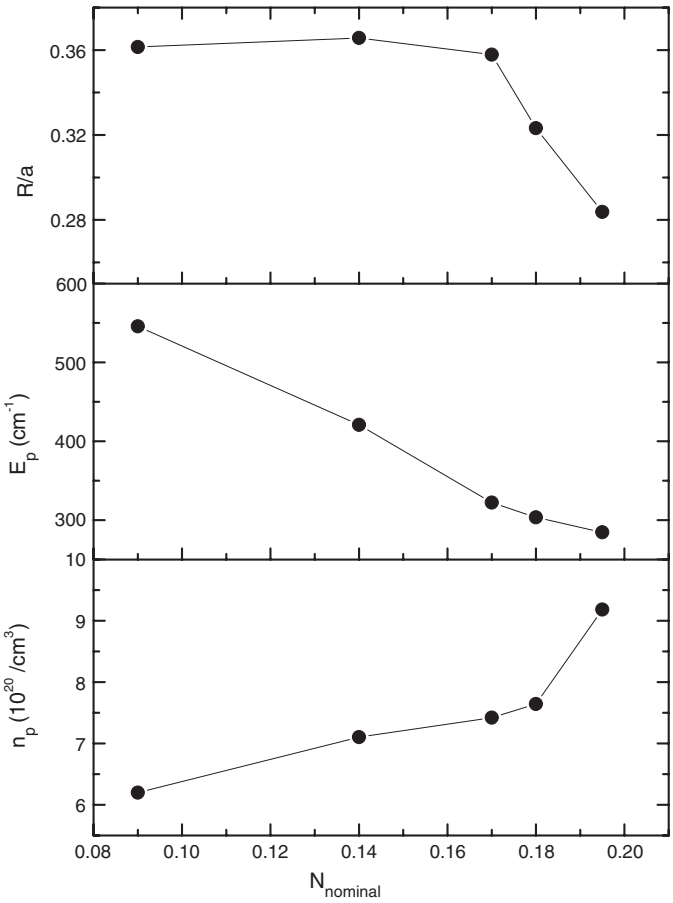

Figure 8. Parameters obtained from fitting the $\mathbf{E} \parallel a$ MIR absorption band of $La_{1-y}Ca_yTiO_{3.4\pm\delta}$ crystals with the large polaron model (equation (2)) as a function of the nominal number of carriers, N_{nominal}: polaron radius R normalized to the lattice parameter a, polaron binding energy E_p, and polaron density n_p.

This would be consistent with a picture of interacting large polarons. However, a discrepancy with a polaronic scenario remains: the polaron radius obtained from the large polaron fits of the MIR band is smaller than the lattice constants. This is in disagreement with the picture of large polarons, whose radii should extend over multiple lattice sites [27]. Interestingly, such a discrepancy was also found in the case of $La_{2/3}Sr_{1/3}MnO_3$ [32], where it could be reconciled by a more sophisticated description taking into account large polarons with finite mass and a finite density of charge carriers. For the present titanate compounds similar modelling is proposed.

In principle, purely electronic excitations could also account for the observed MIR band. It is intriguing to compare our experimental results with the optical response of the closely related perovskite $LaTiO_{3.0}$, which is a Mott–Hubbard insulator with a Ti $3d^1$ electron configuration. For $LaTiO_{3.0}$ the onset of excitations from the lower to the upper Hubbard band was found at around 700 cm^{-1} by optical measurements [20, 36–39, 6]. Upon calcium doping, i.e., hole doping, one observes a transfer of the spectral weight to the region inside the Mott–Hubbard gap, forming a Drude contribution and inner-gap excitations in the form of a MIR band [38, 40, 41], as theoretically predicted [42–44]. Furthermore, for very high doping levels

the initial growth of the inner-gap excitations is expected to be followed by a decrease [43], and the system crosses over from a hole-doped regime to an electron-doped regime [41, 44, 45]. The inset of figure 6 shows the spectral weights of the Drude term and the MIR band for the studied titanates as a function of electron doping. The MIR band shifts towards lower frequencies with increasing electron concentration. The spectral weight of the Drude term and the MIR band increases linearly with increasing electron doping.

Within the picture of the Hubbard model, the studied $La_{1-y}Ca_yTiO_{3.4\pm\delta}$ materials are in a highly hole-doped regime, and the spectral weight evolution is indeed compatible with the Hubbard model in this regime. However, the shift of the MIR band to higher frequencies with decreasing electron (increasing hole) concentration is not consistent with the behaviour expected for the hole doping in Mott–Hubbard systems [40, 41, 44]. One could speculate that this discrepancy is due to the importance of interactions of the charge carriers with the underlying lattice, as was recently suggested for strongly correlated electron systems [46, 47].

In addition to the excitations across the Mott–Hubbard gap, an extremely weak absorption feature in the optical conductivity of $LaTiO_{3.0}$ was found at 0.3 eV (2400 cm^{-1}) [6]. This feature was interpreted in terms of phonon-assisted transitions between the crystal field split Ti t_{2g} levels [6]. In the present $La_{1-y}Ca_yTiO_{3.4\pm\delta}$ compounds, the MIR band in the optical conductivity for $\mathbf{E} \parallel a$ lies in the same range of 0.2–0.4 eV. However, it has a much higher spectral weight than expected for an infrared-forbidden orbital excitation which appears due to broken symmetry. Therefore, such an explanation can be ruled out in the case of the $La_{1-y}Ca_yTiO_{3.4\pm\delta}$ compounds.

Also, an interpretation of the MIR absorption band in terms of 2p–3d charge-transfer transitions should be considered. In other rare-earth titanates the absorption bands due to charge-transfer excitations are observed at around 4 eV [37, 39, 48], i.e., at much higher energies compared to the frequency position of the absorption band in $La_{1-y}Ca_yTiO_{3.4\pm\delta}$. On the other hand, recently the one-electron approach to the charge-transfer states was pointed out to be an insufficient, oversimplified picture, and energies for many-electron charge-transfer transitions were obtained using a cluster approach [49]. It was shown that the charge-transfer transitions can occur at much lower energies, and could thus in principle serve as a possible explanation for the observed MIR bands along the a and b direction. Within this picture, shifts of the charge transfer transitions with calcium doping are expected, since the induced changes of the crystal structure (see discussion of the phonon spectra) alters the electronic band structure. However, the temperature dependence of the MIR band in the optical conductivity of $LaTiO_{3.41}$ is relatively strong [8], which renders an interpretation of the MIR band in terms of charge-transfer excitations less likely.

Thus, among the possible explanations for the MIR band in the $La_{1-y}Ca_yTiO_{3.4\pm\delta}$ compounds, purely electronic excitations—like Mott–Hubbard inner-gap states, local crystal field excitations, and charge-transfer excitations—appear to be unlikely. The observed shift of the MIR band with doping is best explained within a polaronic model.

Finally, we want to comment on the optical properties of the insulating material $La_{0.8}Ca_{0.2}TiO_{3.40}$. In contrast to the other studied $La_{1-y}Ca_yTiO_{3.4\pm\delta}$ compounds, the $\mathbf{E} \parallel a$ optical conductivity spectrum does not contain a MIR absorption band. Also, the absorption feature located at around 6000 cm^{-1} for $\mathbf{E} \parallel b$ is not observed and $La_{0.8}Ca_{0.2}TiO_{3.40}$ appears to be less anisotropic concerning its optical response. These findings suggest significant differences in the crystal structure compared to the other studied titanates. This is corroborated by the observed differences in the phonon spectra. Since among all studied titanates no major differences in the lattice parameters exist (see table 1), the structural differences should be on a local scale; for example, the degree of distortion of the TiO_6 octahedra might be altered.

5. Summary

In conclusion, the effects of doping on the polarization-dependent optical properties of $La_{1-y}Ca_yTiO_{3.4\pm\delta}$ crystals were studied at room temperature. The optical conductivity of all studied titanates with $y < 0.2$ demonstrates a quasi-1D conducting character. The optical conductivity spectra along the chain direction consist of a Drude-like peak superimposed by phonon lines and a strong MIR band. The vibrational modes exhibit small changes with calcium doping, suggesting small changes in the effective charge, bond lengths, or octahedral distortions induced by the substitution of trivalent lanthanum with divalent calcium. The MIR band observed along the conducting direction exhibits a shift to lower energies with increasing electron density. Among various models (polaronic, Mott–Hubbard, crystal field, and charge-transfer excitations), this band is best described in terms of a polaron model.

Acknowledgments

We thank G Untereiner for valuable technical help. Fruitful discussions with H Winter, M Dressel, and S Schuppler are acknowledged. This work was financially supported by the BMBF (project No 13N6918A) and the Deutsche Forschungsgemeinschaft.

References

[1] Hemberger J, Krug von Nidda H-A, Fritsch V, Deisenhofer J, Lobina S, Rudolf T, Lunkenheimer P, Lichtenberg F, Loidl A, Bruns D and Büchner B 2003 *Phys. Rev. Lett.* **91** 066403
[2] Cwik M, Lorenz T, Baier J, Müller R, André G, Bourée F, Lichtenberg F, Freimuth A, Schmitz R, Müller-Hartmann E and Braden M 2003 *Phys. Rev.* B **68** 060401
[3] Mochizuki M and Imada M 2004 *New J. Phys.* **6** 154
[4] Ulrich C, Gössling A, Grüninger M, Guennou M, Roth H, Cwik M, Lorenz T, Khaliullin G and Keimer B 2005 Orbital excitations in titanates *Preprint* cond-mat/0503106 and references therein
[5] Loa I, Wang X, Syassen K, Roth H, Lorenz T, Hanfland M and Mathis Y-L 2005 Pressure-driven orbital reorientation and change in Mott–Hubbard gap in $YTiO_3$ *Preprint* cond-mat/0504383
[6] Rückamp R, Benckiser E, Haverkort M W, Roth H, Lorenz T, Freimuth A, Longen L, Möller A, Meyer G, Reutler P, Büchner B, Revcolevschi A, Cheong S-W, Sekar C, Krabbes G and Grüninger M 2005 *New J. Phys.* **7** 144
[7] Lichtenberg F, Herrnberger A, Wiedenmann K and Mannhart J 2001 *Prog. Solid State Chem.* **29** 1
[8] Kuntscher C A, van der Marel D, Dressel M, Lichtenberg F and Mannhart J 2003 *Phys. Rev.* B **67** 035105
[9] Frank S, Kuntscher C A, Loa I, Syassen K and Lichtenberg F 2006 *Phys. Rev.* B **74** 054105
[10] Kuntscher C A, Frank S, Loa I, Syassen K, Lichtenberg F, Yamauchi T and Ueda Y 2006 *Infrared Phys. Technol.* **49** 88–91
[11] Presura C, Popinciuc M, van Loosdrecht P H M, van der Marel D, Mostovoy M, Yamauchi T and Ueda Y 2003 *Phys. Rev. Lett.* **90** 026402
[12] Kuntscher C A, Frank S, Loa I, Syassen K, Yamauchi T and Ueda Y 2005 *Phys. Rev.* B **71** 220502(R)
[13] Wang N L, Clayman B P, Mori H and Tanaka S 2003 *J. Phys.: Condens. Matter* **12** 2867
[14] Thomas G A, Rapkine D H, Cooper S L, Cheong S-W, Cooper A S, Schneemeyer L F and Waszczak J V 1992 *Phys. Rev.* B **45** 2474
[15] Calvani P, Capizzi M, Lupi S, Maselli P, Paolone A and Roy P 1996 *Phys. Rev.* B **53** 2756
[16] Lupi S, Maselli P, Capizzi M, Calvani P, Giura P and Roy P 1999 *Phys. Rev. Lett.* **83** 4852
[17] Daniels P, Lichtenberg F and van Smaalen S 2003 *Acta Crystallogr.* **59** i15
[18] Lichtenberg F, unpublished
[19] Kuntscher C A, unpublished
[20] Lunkenheimer P, Rudolf T, Hemberger J, Pimenov A, Tachos S, Lichtenberg F and Loidl A 2003 *Phys. Rev.* B **68** 245108
[21] Last J T 1957 *Phys. Rev.* **105** 1740
[22] Atkins P W 1986 *Physical Chemistry* (Oxford: Oxford University Press) p 455
[23] Crandles D A, Timusk T, Garrett J D and Greedan J E 1994 *Phys. Rev.* B **49** 4299

[24] Lixin He, Neaton J B, Vanderbilt D and Cohen M H 2003 *Phys. Rev.* B **67** 012103
[25] Cockayne E and Burton B P 2000 *Phys. Rev.* B **62** 3735
[26] Ghosez Ph, Michenaud J-P and Gonze X 1998 *Phys. Rev.* B **58** 6224
[27] Emin D 1993 *Phys. Rev.* B **48** 13691
[28] Cataudella V, De Filippis G and Iadonisi G 1999 *Eur. Phys. J.* B **12** 17
[29] Calvani P 2001 Optical properties of polarons *Riv. Nuovo Cimento* **24** 1–71
[30] Fratini S and Quémerais P 1998 *Mod. Phys. Lett.* B **12** 1003
[31] Tempere J and Devreese J T 2001 *Phys. Rev.* B **64** 104504
[32] Hartinger Ch, Mayr F, Deisenhofer J, Loidl A and Kopp T 2004 *Phys. Rev.* B **69** 100403(R)
[33] Hartinger Ch, Mayr F, Loidl A and Kopp T 2004 Polaronic excitations in CMR manganite films *Preprint* cond-mat/0406123
[34] Reik H G 1963 *Phys. Rev. Lett.* **5** 236
[35] Bi X-X, Eklund P C and Honig J M 1993 *Phys. Rev.* B **48** 3470
[36] Crandles D A, Timusk T, Garrett J D and Greedan J E 1992 *Physica* C **201** 407
[37] Arima T, Tokura Y and Torrance J B 1993 *Phys. Rev.* B **48** 17006
[38] Okimoto Y, Katsufuji T, Okada Y, Arima T and Tokura Y 1995 *Phys. Rev.* B **51** 9581
[39] Arima T and Tokura Y 1995 *J. Phys. Soc. Japan* **64** 2488
[40] Katsufuji T, Okimoto Y and Tokura Y 1995 *Phys. Rev. Lett.* **75** 3497
[41] Taguchi Y, Tokura Y, Arima T and Inaba F 1993 *Phys. Rev.* B **48** 511
[42] Stephan W and Horsch P 1990 *Phys. Rev.* B **42** 8736
[43] Dagotto E, Moreo A, Ortolani F, Riera J and Scalapino D J 1992 *Phys. Rev.* B **45** 10107
[44] Jarrell M, Freericks J K and Pruschke Th 1995 *Phys. Rev.* B **51** 11704
[45] Dagotto E, Moreo A, Ortolani F, Poilblanc D and Riera J 1992 *Phys. Rev.* B **45** 10741
[46] Sangiovanni G, Capone M, Castellani C and Grilli M 2005 *Phys. Rev. Lett.* **94** 026401
[47] Koller W, Hewson A C and Edwards D M 2005 *Phys. Rev. Lett.* **95** 256401
[48] Fujishima Y, Tokura Y, Arima T and Uchida S 1992 *Phys. Rev.* B **46** 11167
[49] Zenkov A V 2004 *Phys. Status Solidi* b **241** 2508